PAPER

Check for updates

High yield production of 1,4-cyclohexanediol and 1,4-cyclohexanediamine from high molecular-weight lignin oil†

Xianyuan Wu, [ID] [a] Mario De bruyn,[c] Julia Michaela Hulan,[c] Henrique Brasil,[c] Zhuohua Sun[b] and Katalin Barta [ID] *[a,c]

The complete utilization of all lignin depolymerization streams obtained from the reductive catalytic fractionation (RCF) of woody biomass into high-value-added compounds is a timely and challenging objective. Here, we present a catalytic methodology to transform beech lignin-derived dimers and oligomers (DO) into well-defined 1,4-cyclohexanediol and 1,4-cyclohexanediamine. The latter two compounds have vast industrial relevance as monomers for polymer synthesis as well as pharmaceutical building blocks. The proposed two-step catalytic sequence involves the use of the commercially available RANEY® Ni catalyst. Therefore, the first step involves the efficient defunctionalization of lignin-derived 2,6-dimethoxybenzoquinone (DMBQ) into 1,4-cyclohexanediol (14CHDO) in 86.5% molar yield, representing a 10.7 wt% yield calculated on a DO weight basis. The second step concerns the highly selective amination of 1,4-cyclohexanediol with ammonia to give 1,4-cyclohexanediamine (**14CHDA**) in near quantitative yield. The ability to use RANEY® Ni and ammonia in this process holds great potential for future industrial synthesis of 1,4-cyclohexanediamine from renewable resources.

Introduction

Currently, a high demand exists for the development of sustainable catalytic methodologies for known commodity chemicals from renewable resources such as lignocellulosic biomass.[1–11] In this respect, reductive catalytic fractionation (RCF) is a powerful tool to catalytically fractionate lignocellulosic biomass.[12–15] Typically, this results in the depolymerization of lignin into monomeric and oligomeric fractions while largely retaining the structural integrity of the cellulose component. Recent research attention is given to the valorization of the oligomeric lignin fraction as its further deconstruction would greatly enhance the overall achievable monomeric yield. In this respect, the group of Samec recently developed an elegant oxidative process to convert part of the oligomeric lignin fraction featuring distinct C–C linkages obtained upon

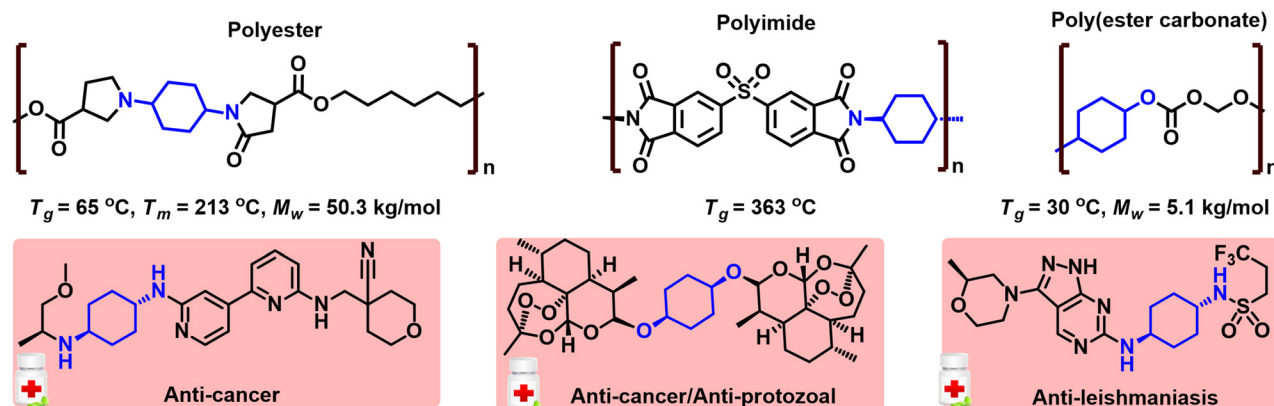[a]*Stratingh Institute for Chemistry, University of Groningen, Groningen, The Netherlands*
[b]*Beijing Key Laboratory of Lignocellulosic Chemistry, Beijing Forestry University, No. 35 Tsinghua East Road Haidian District, Beijing, 100083, P. R. China*
[c]*Department of Chemistry, Organic and Bioorganic Chemistry, University of Graz, Heinrichstrasse 28/II, 8010 Graz, Austria. E-mail: katalin.barta@uni-graz.at*
†Electronic supplementary information (ESI) available. See DOI: https://doi.org/10.1039/d2gc03777g

RCF to 2,6-dimethoxybenzoquinone (DMBQ),[16] a compound with wide synthetic applications.[17]

Here, we present the development of feasible catalytic strategies to convert DMBQ into industrially highly relevant and well-defined 1,4-cyclohexanediol (14CHDO) and 1,4-cyclohexanediamine (**14CHDA**). 14CHDO is a valuable compound that has been shown to be useful as a monomer to produce polycarbonates, polyethers and polyesters including scratch-resistant coatings as well as supramolecular associations owing to the distinct *cis/trans* isomerism of this molecule (Fig. 1A).[18–21] 14CHDO serves as a direct synthetic precursor to a range of pharmaceuticals, typically by the functionalization of one or both hydroxyl groups.[22] Exemplary in this respect are the synthetic routes to phenyl cyclohexylcarboxamides, dihydroartemisinin and derivatives, and compounds with distinct anticancer properties.[22] 14CHDO is also the prime industrial precursor to 1,4-cyclohexanedione,[23] a highly versatile platform molecule for the production of pharmaceuticals such as the analgesic Cebranopadol.[24,25] The prime applications of diamines such as **14CHDA** are in the preparation of polyamides,[26,27] polyimides,[28] polyureas,[29] polyurethanes[30] and biologically active compounds (Fig. 1A).[31,32]

Industrially, 14CHDO and **14CHDA** are produced from fossil resources, relying on the use of benzene, a carcinogenic and mutagenic compound with a lengthy hazard classification, by several strategies that are briefly summarized in Fig. 1B and

A. Applications of 14CHDO and 14CHDA for the production of polymers and pharmaceuticals

B. Mostly common industrial routes to 14CHDO and 14CHDA
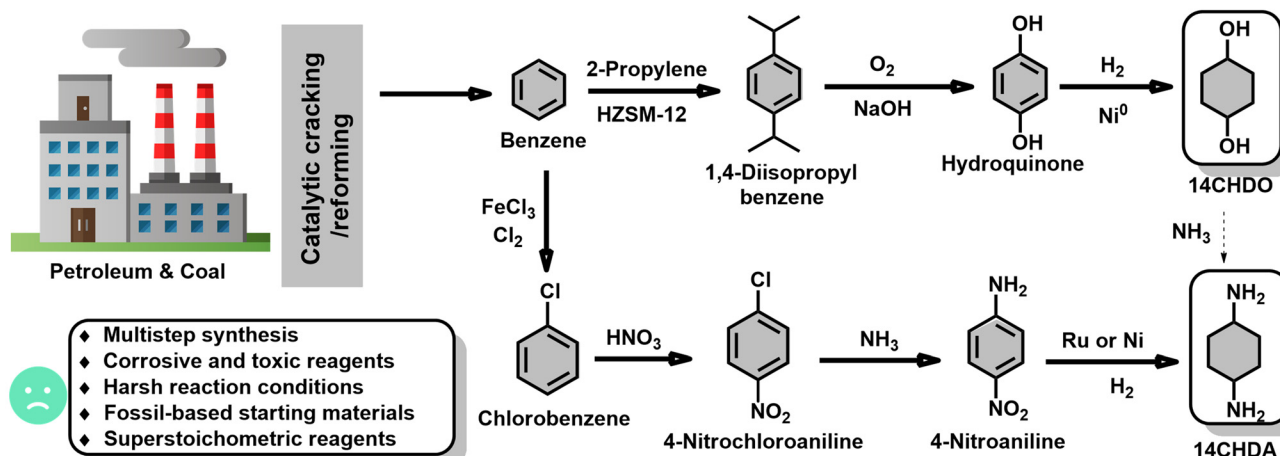
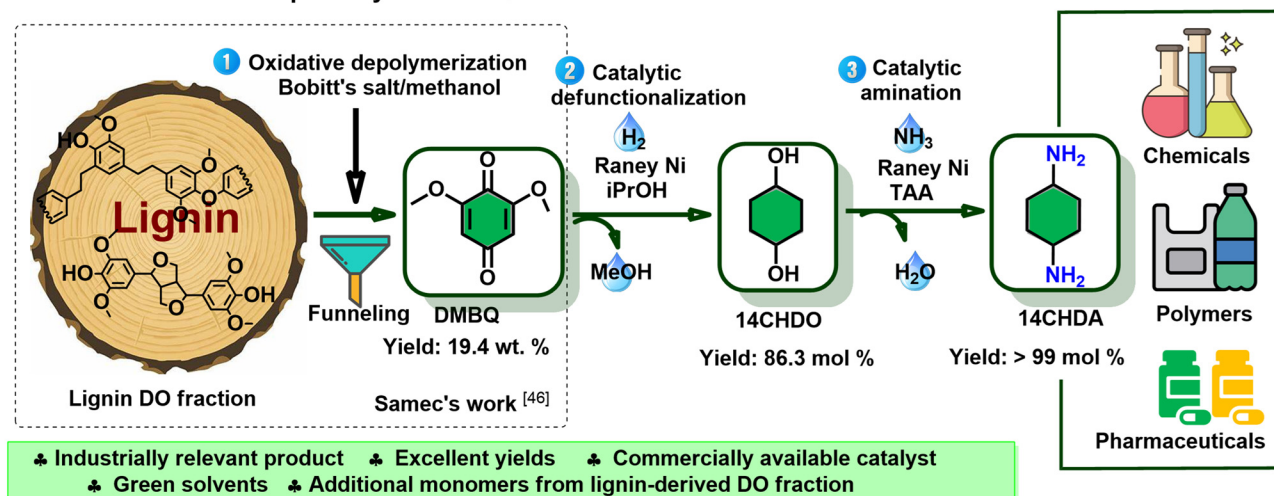**C. Alternative sustainable pathway to 14CHDO and 14CHDA**

Fig. 1   Existing and potential future strategies to produce 14CHDO and **14CHDA**. (A) Applications of 14CHDO and **14CHDA** for the production of polymers and pharmaceuticals; (B) Traditional industrial and prospective pathways for the production of 14CHDO and **14CHDA**, with the central starting compound being fossil-derived benzene. More details can be found in ESI Note 1.† (C) Here proposed and developed three-step catalytic pathway to 14CHDO and **14CHDA** from lignocellulosic biomass: (1) Oxidative cleavage of the RCF oligomeric lignin fraction to DMBQ using Bobbit's salt.[16] (2) Demethoxylation and hydrogenation of DMBQ to 14CHDO over RANEY® Ni catalyst. (3) Catalytic amination of 14CHDO to **14CHDA** over RANEY® Ni catalyst.

explained in ESI Note 1† in more detail.[33] Central to the synthesis of 14CHDO is the formation of hydroquinone (HQ),[34] while **14CHDA** can be prepared by hydrogenation of 1,4-phenylenediamine (14PDA).[35,36] However, these processes have specific drawbacks such as multi-step synthesis routes and the use of super stoichiometric reagents under harsh reaction conditions.

In this work, we present a catalytic alternative (Fig. 1C) that starts from lignin-derived depolymerization streams and relies on a two-step RANEY® Ni based sequence capable of converting DMBQ into **14CHDA**. More specifically, the first step comprises the reductive demethoxylation and hydrogenation of DMBQ into 14CHDO in up to 86.5% yield, while the second step features a near-quantitative amination of 14CHDO into **14CHDA** in the presence of ammonia. The latter transformation fits the quest for sustainable catalytic methodologies to introduce nitrogen in biomass-derived chemicals.[37–49] To illustrate the robustness of this method, we also show that 10.7 wt% 14CHDO (based on a DO fraction basis) can be derived from a real RCF oligomeric lignin fraction.

Results and discussion

Catalytic demethoxylation and hydrogenation of DMBQ to 14CHDO

Firstly, the demethoxylation/hydrogenation of DMBQ to 14CHDO was tested using a range of commercially available heterogeneous noble/non-noble catalysts (Fig. 2A and Table S1†) under standard reaction conditions: DMBQ, RANEY® Ni, 170 °C, 4 h, iPrOH, 10 mg dodecane. It was found that Pd/C and Pd/Al$_2$O$_3$ engaged predominantly in the hydrogenation of the aromatic ring, producing a high yield of the compound 2,6-dimethoxycyclohexane-1,4-diol (**3A**). This preferred catalytic hydrogenation of the aromatic ring has been demonstrated earlier.[50,51] While these two catalysts do display some reductive demethoxylation capability, giving 2-methoxycyclohexane-1,4-diol (**4A**) in the yields of 9.2 and 16.2%, respectively, their effective selectivity to 14CHDO remained nonetheless low, 4.4 and 12.2%, respectively. Changing the active metal from Pd to Ru led to a sizeable increase in the **4A** and 14CHDO selectivities. The best results were obtained with Ru/Al$_2$O$_3$ as the catalyst, showing a 14CHDO selectivity of 55.3%. However, under the given reaction conditions, the Ru/Al$_2$O$_3$ catalyst also engaged in hydrodeoxygenation, leading to the formation of cyclohexanol (**5A**) in 15% yield. Additionally, three heterogeneous Ni-containing catalysts were tested, namely Ni/SiO$_2$, Ni/SiO$_2$–Al$_2$O$_3$ and RANEY® Ni. From Fig. 2A and Table S1,† it can be inferred that Ni/SiO$_2$ delivers a good, 50.4% 14CHDO yield, higher than that obtainable with Ni/SiO$_2$–Al$_2$O$_3$ (39.4%). Gratifyingly, in the presence of RANEY® Ni, the 14CHDO yield increased to 65.9%. The higher catalytic activity of RANEY® nickel was attributed to its excellent hydrogen transfer activity when using isopropanol as the H-donor solvent.[52] It is noteworthy that none of the tested Ni catalysts engaged in hydrodeoxygenation, with only low levels of

14CHDO being detected. These results are in line with the work published by the Rinaldi group.[52] It is further noteworthy that our RANEY® Ni process yields *cis/trans* 14CHDO in a 40/60 ratio (for ^{1}H NMR results, see ESI section 2.4†). In contrast, the hydrogenation of hydroquinone to 14CHDO leads to a 3 : 1 excess of the *cis vs. trans* isomer over a Ni-Sr/γ-Al$_2$O$_3$ catalyst.[53]

Having established the superiority of the RANEY® Ni catalyst, the influence of the solvent was investigated next (Fig. 2B and Table S2†). Using MeOH as the solvent showed near-exclusive 2,6-dimethoxybenzene-1,4-diol (**1A**) formation (*i.e.*, DMBQ aromatization), while usage of EtOH gave a blend of **1A**, **3A**, **4A**, and 14CHDO, thus pointing at a somewhat more developed demethoxylation/hydrogenation capability. The limited demethoxylation and hydrogenation capability of RANEY® Ni in the presence of MeOH or EtOH likely relates to the strong adsorption of methyl- and ethyl-alcoholates on the surface of the RANEY® Ni catalyst.[52,54,55] Interestingly, increasingly better 14CHDO selectivity was obtained when increasing the hydrophobicity and bulkiness of the alcohol solvent. Indeed, in going from propanol to isopropanol, the 14CHDO selectivity increased from 24.9 to 65.9%, while still forming sizeable amounts of **4A** (respectively, 39.4% and 30.2%). Isopropanol has shown to be a good partner with RANEY® nickel in the demethoxylation and hydrogenation of aromatic rings compared to other simpler alcohols (methanol, ethanol *etc.*).[52] Further suppression of **4A** formation could be achieved when using *t*-amyl alcohol as the solvent with a selectivity of 25.2%, yet no further advance in 14CHDO selectivity (62%) could be observed. Aside from alcoholic solvents, 2-MeTHF and water were tested. From Fig. 2C, it can be inferred that 2-MeTHF gives similar results in terms of 14CHDO selectivity (63.4%) as observed with *t*-amyl alcohol, but both selectivity values were slightly lower than those (65.9%) in isopropanol. In the presence of water, the observed 14CHDO selectivity falls out lower than that observed with *t*-amyl alcohol and 2-MeTHF, reaching 52.8%.

By adopting isopropanol as the reaction solvent, the influence of the reaction temperature was investigated. Fig. 2C (Table S3†) shows a direct proportionality between the attained 14CHDO selectivity and the reaction temperature with the best 14CHDO selectivity (85.2%) obtained at 190 °C. Advances beyond 190 °C led to a significant formation of **5A** and cyclohexane (**6A**), a set of hydrodeoxygenation products directly derived from the target 14CHDO product. The influence of the reaction time was conveniently assessed at 170 °C. From Fig. 2D (Table S4†), it can be seen that the obtainable 14CHDO selectivity increases with reaction time, and the optimal value centers around the 12–14 h mark with 14CHDO selectivities of 84–86.3%. Applying longer reaction times led to decreased 14CHDO selectivities as the hydrodeoxygenation of 14CHDO to **5A**/**6A** became ever more dominant.

With the DMBQ-to-14CHDO reaction featuring multiple (potential) simultaneous/consecutive reaction steps, among hydrogenation, demethoxylation and hydrodeoxygenation, we performed a concise study to reveal the main reaction pathway. This is achieved by combining the above gained insights with
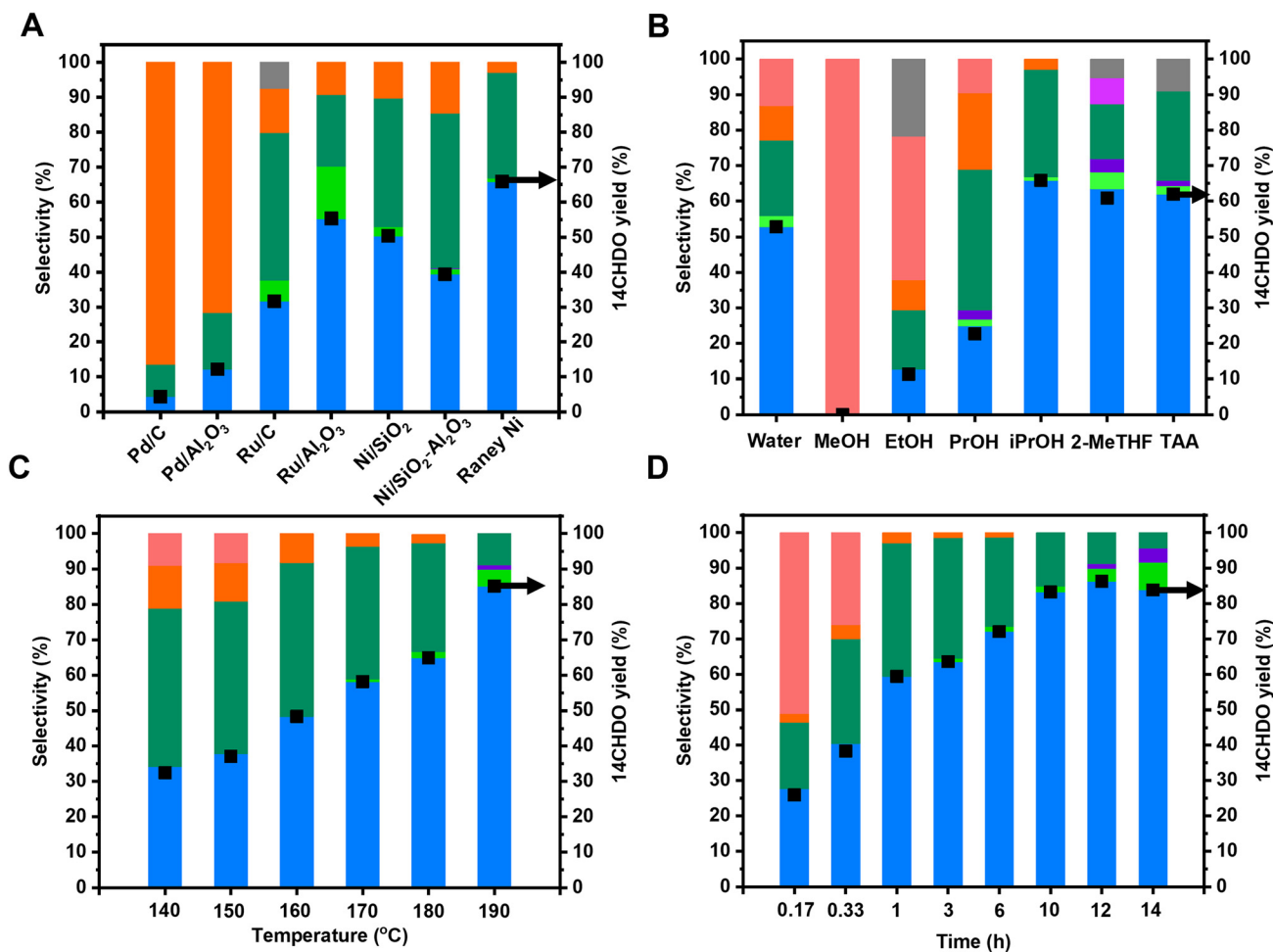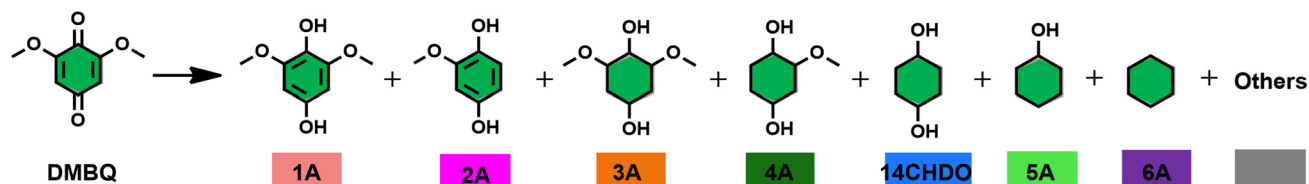
Fig. 2 Establishment of the optimal reaction conditions for the catalytic conversion of DMBQ to 14CHDO (A–D); Unless otherwise specified, standard reaction conditions are used: DMBQ (1 mmol, 0.200 g), 200 mg RANEY® Ni, 170 °C, 4 h, 15 mL solvent, 10 mg dodecane. Screening of (A) commercially available heterogeneous metal catalysts. The metal loading of the noble metal catalyst is 5 wt%, while it is 65 wt% for Ni/SiO$_2$ and Ni/SiO$_2$– Al$_2$O$_3$ and 89 wt% for RANEY® Ni; (B) solvent influence; (C) reaction temperature, 2 h; (D) different reaction time; (A–D). The numerical values are given in the ESI and more specifically Tables S1–S4.† Conversion and yield values were determined by GC-FID using calibration curves and an internal standard; The black square symbol refers to the yield of 14CHDO.

a series of probe reactions on individual compounds, such as DMBQ, **1A**, **2A**, **3A**, **4A** and 14CHDO (Fig. 3A–F, and Tables S5– S10†). In addition, in order to shed light on the reaction mechanism, reaction kinetics were analysed to describe how **2A** was transformed into **5A**, following a pseudo-homogeneous kinetics model. To simplify the model, the following assumptions were made: (1) the concentration of H$_2$ in the liquid phase is constant and the adsorption of H$_2$ is the most relevant on the catalyst surface. (2) Compound **HQ** is rapidly consumed after its production and was treated as an intermediate. (3) The product **HQ** was not detected in significant amounts.

Thus, $k_4 \gg k_2$. Based on the assumptions detailed above, the model could be simplified to a power-law model, where k_n are the apparent kinetic constants. The resulting system of ordinary differential equations is the following:

$$\frac{d[HQ]}{dt} = k_2[2A] - k_4[HQ] = 0$$

$$\frac{d[2A]}{dt} = -(k_1 + k_2)[2A]$$

$$\frac{d[4A]}{dt} = k_1[2A] - k_3[4A]$$

$$\frac{d[HQ]}{dt} = k_2[2A] - k_4[HQ]$$

$$\frac{d[14CHDO]}{dt} = k_3[4A] + k_4[HQ]$$

The overall reaction scheme is outlined in Fig. 3G and further discussed below. Firstly, it was found that the DMBQ to 14CHDO reaction occurs chiefly over the **1A** intermediate (Fig. 3A). Moreover, it could also be established that the DMBQ to **1A** reaction occurs readily in the presence of RANEY® Ni already at RT. Further key findings related to the reaction network were that the rate of the HQ to 14CHDO transformation is orders of magnitude higher than the 4A to 14CHDO transformation (respectively, 2.9 min^{-1} ↔ 3.73 × 10^{-10} min^{-1}) (Fig. 3F and E) and the reaction rates of the **2A** to **4A** and **2A** to HQ reactions (respectively, 4.57 × 10^{-3} min^{-1} and 6.01 × 10^{-3} min^{-1}) (Fig. 3C). These two observations combined with the notion that the transformation of **3A** to **4A** (14CHDO) is very slow (Fig. 3D) establish the preferred reaction mechanism as DMBQ → **2A** → HQ → 14CHDO. Details of the determination of the rate-determining steps can be found in ESI section 2.3.†

Catalytic demethoxylation and hydrogenation of the lignin-derived DO fraction to 14CHDO

Having identified the optimal reaction conditions, their validity was tested towards the conversion of the oligomers in a real lignin oil obtained from beech wood, a hardwood species. To this end, beech wood was converted into a suitable lignin oil by following a published procedure by Samec.[16] The details of this procedure are explicitly outlined in ESI section 2.5† and are also depicted in Fig. 4A. Importantly, the oil was subjected to DCM/water partitioning, thereby removing the saccharides, followed by fractional distillation of the DCM phase (1 mbar, 220 °C, 0.5 h). The latter operation resulted in two distinct fractions, namely: (1) low molecular-weight lignin-derived monomers, predominantly with 2,6-dimethoxy-4-(propenyl)phenol (**1S′**) and 4-propylsyringol (**1S**) signature (total 24.6 mg) and (2) a higher molecular-weight fraction predominantly displaying β-1 and β–β linkages (shown in HSQC – Fig. S14†) and containing mainly lignin dimers and oligomers (total 66.6 mg). The analysis of the latter fraction was also performed by GC-FID/MS (Fig. S9†) and GPC (Fig. S12†), with the latter characterization technique revealing an average oligomer molecular weight (M_w) of 1480 g mol^{-1}. Catalytic oxidative cleavage of the dimeric and oligomeric lignin fractions was performed using commercially available Bobbitt's salt, thereby introducing a relevant amount of DMBQ into the lignin oil *i.e.*, 19.4 wt% DMBQ *vis-à-vis* the original dimeric and oligomeric lignin fractions. Eliminating all reduced Bobbitt's salt *via* filtration by means of a short silica gel column (1 vol% MeOH in DCM) gave **Crude 1**, the characterization of which was performed by GC-FID/MS (Fig. S10†), GPC (M_w = 321 g mol^{-1}, M_n = 189 g mol^{-1}) (Fig. S13†) and HSQC (Fig. S15†). This concisely

showed the decomposition of the lignin-derived oligomers into DMBQ. Using the here developed RANEY® Ni catalysed methodology, it was possible to demethoxylate/hydrogenate the DMBQ contained in **Crude 1**, yielding 14CHDO (10.7 wt%) containing **Crude 2**. Characterization of **Crude 2** was performed by GC-FID/MS (Fig. S11†) and HSQC (Fig. S16†), thereby unequivocally confirming the conversion of DMBQ to 14CHDO.

To illustrate the generality of this methodology, birch, poplar, and oak lignocellulose (500 mg each) were also subjected to the same catalytic protocol treatment (Fig. 4B), giving the respective 14CHDO yields of 7.1 wt%, 7.3 wt% and 7.3 wt% on DO basis as shown in Fig. 4C.

Catalytic direct amination of 14CHDO to 14CHDA

Next, the catalytic direct coupling of 14CHDO with ammonia to **14CHDA** *via* a hydrogen-borrowing methodology was investigated. Firstly, the influence of a range of commercially available (heterogeneous) metal catalysts was assessed. It was found that Ru and Ni based catalysts display no meaningful reactivity towards this transformation, while Pd catalysts actively engaged in the formation of aniline (**2B**) (>80% selectivity) over the target product **14CHDA** (Fig. 4A, and Table S11†) and phenol (**1B**). Uniquely, of all tested commercially available heterogeneous metal catalysts, only the use of RANEY® Ni led to the formation of **14CHDA** in high yield (up to 85%), the main side product being the mono-aminated product 4-amino-cyclohexanol (**3B** – 15% yield). This unique catalytic ability of RANEY® Ni was attributed to its distinct capability of engaging in all the relevant reaction steps to the hydrogen borrowing sequence: alcohol dehydrogenation and imine reduction. High-loading of catalyst is required because RANEY® Ni occurs as a mixture of metallic nickel and inactive nickel oxide nickel as well as inaccessible Ni in the bulk of the catalyst. Also, commercial wet RANEY® nickel used in the here-presented amination contains a substantial amount of water (~20 wt%). Surprisingly though, isolation of **14CHDA** from such a mixture (mainly **14CHDA** and **3B**) by either column chromatography or (HCl) salt formation was found to be particularly challenging. Fortunately, dedicated optimization of the reaction temperature (Fig. 4C and Table S13†) and the reaction time (Fig. 4D and Table S14†) revealed conditions (170 °C and 8 h) under which **14CHDA** was formed in near quantitative yield. From a solvent perspective, it could be further established that the use of *t*-amyl alcohol and toluene was most beneficial for the 14CHDO to **14CHDA** transformation (Fig. 4B and Table S12†). As observed during the **14CHDA** formation, the use of MeOH as the solvent gave no noticeable conversion. Using water as the solvent gave a mixture of **14CHDA** (25%) and **4B** (75%) with a conversion of 64%. The specific use of 25 wt% NH$_3$ in H$_2$O led to the preferential formation of the mono-aminated product **3B** and the **4B** dimer in line with the literature.[37,55,56] Of particular interest is the distinct change in isomeric ratio upon going from 14CHDO to **14CHDA**. Indeed, while 14CHDO with a *cis/trans* 58 : 42 mixture was subjected to amination, **14CHDA** was obtained with a 25 : 75 *cis/trans* ratio,
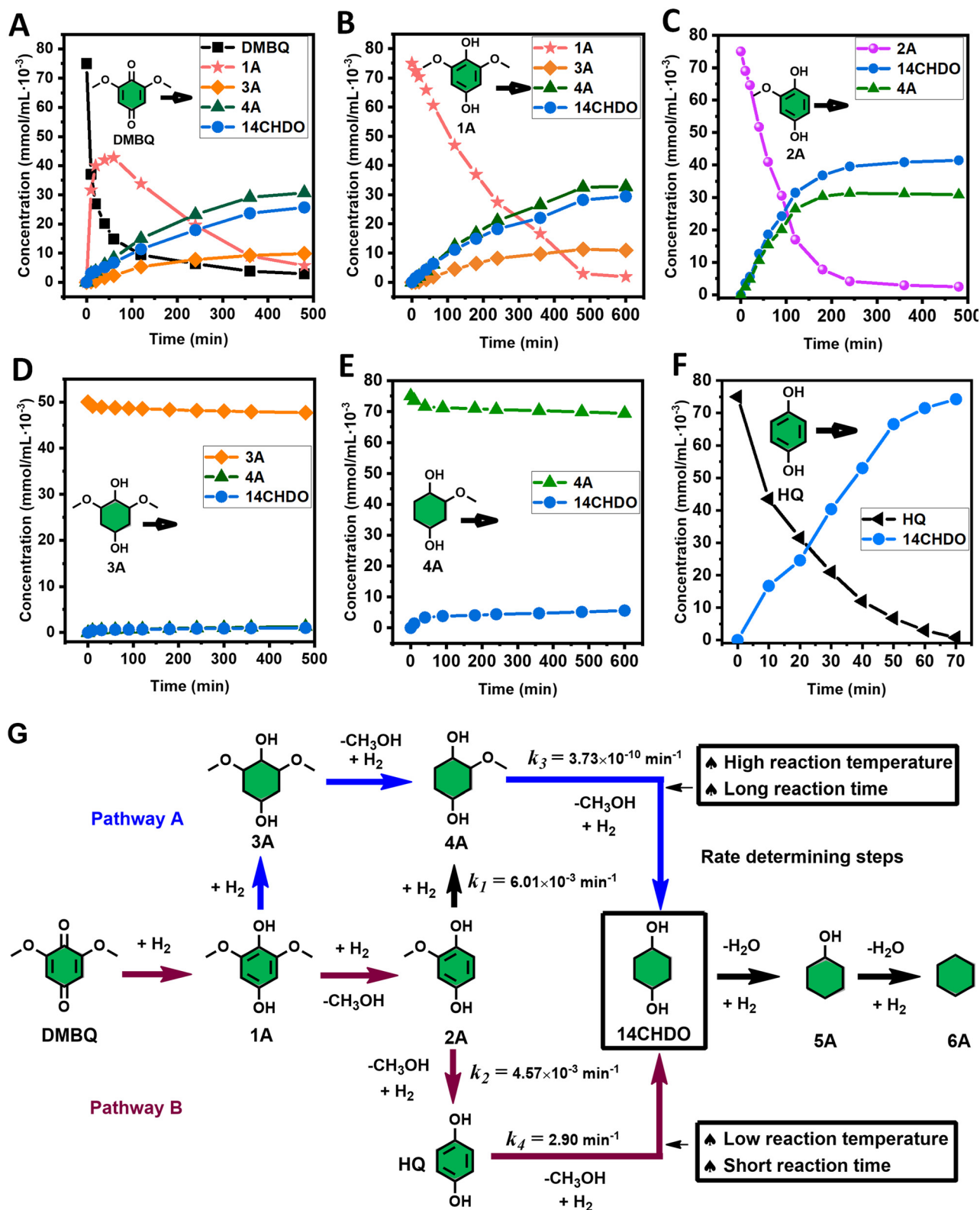
Fig. 3 Elucidation of the reaction pathway by means of the reaction kinetics analysis. Reaction conditions: 1.5 mmol substrate, 30 mg RANEY® Ni catalyst, 170 °C, 0–600 min, 20 mL isopropanol, 10 mg dodecane; (A–F) The numerical values for this assessment can be found in the ESI and more specifically in Tables S5–S10.† (D) 1 mmol **3A**, 15 mg catalyst (G) proposed reaction network: k_1, k_2, k_3 and k_4 are the apparent kinetic constants obtained from data fitting with a pseudo-homogeneous power-law model.
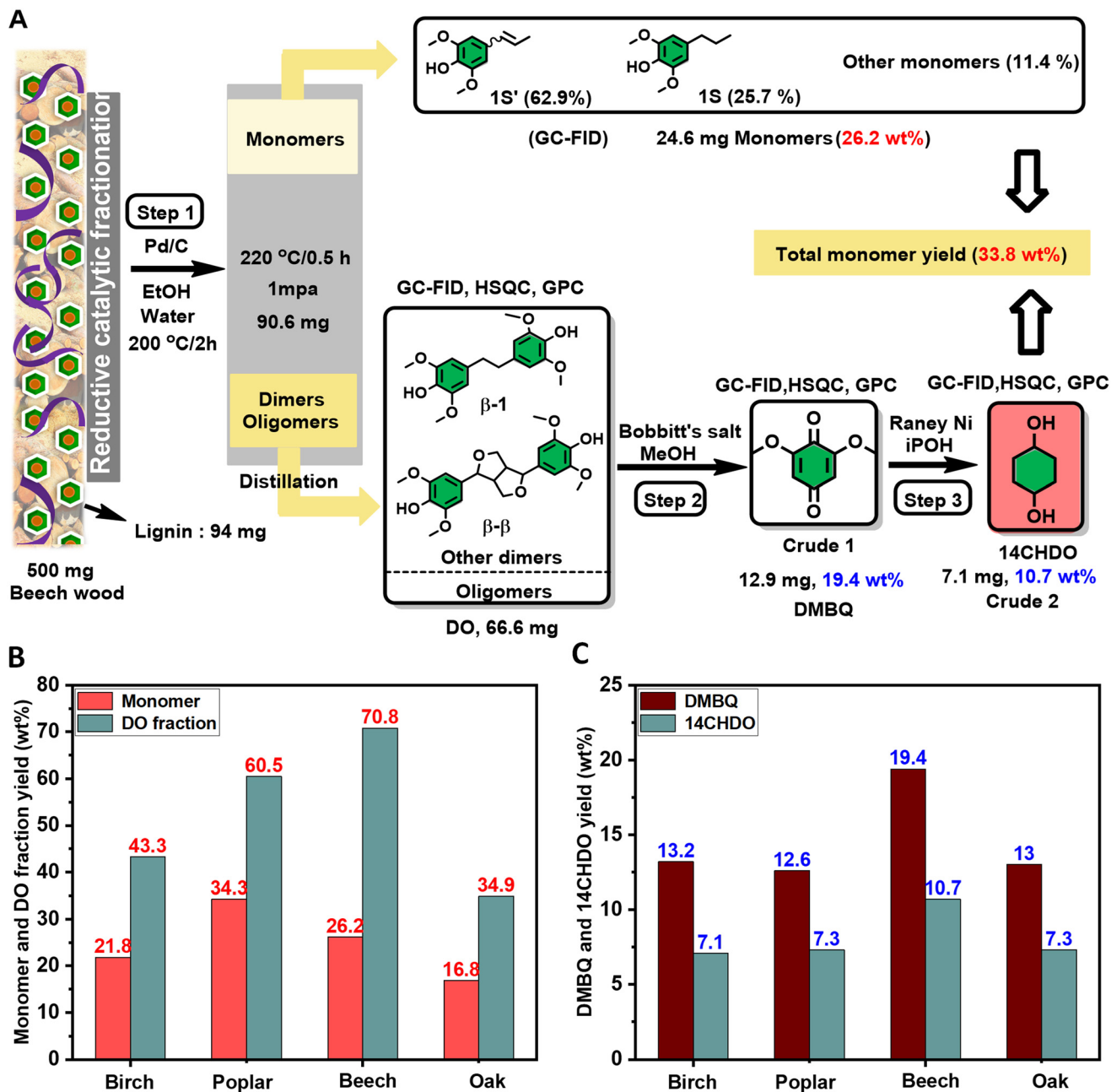
Fig. 4 An overview toward the production of 14CHDO from different types of lignocellulose. (A) Step 1: RCF of beech wood produced crude lignin oil (500 mg beech wood, 50 mg Pd/C catalyst, 12 mL ethanol/12 mL water, 200 °C, 2 h) followed by DCM/water partitioning to eliminate the saccharide content; Step 2: Catalytic oxidative deconstruction of the dimeric and oligomeric lignin fraction into **DMBQ** using Bobbitt's salt. (66.6 mg **DO** fraction, 264 mg Bobbitt's salt, 7 ml methanol, 0.4 wt% water relative to methanol, 100 °C, 0.5 h); Step 3: Catalytic demethoxylation and hydrogenation of **Crude 1** into **14CHDO** over RANEY® Ni catalyst. (**Crude 1**, 200 mg RANEY® Ni, 15 mL isopropanol, 30 bar H$_2$, 170 °C, 10 h). The red-colored yield values were determined on a lignin basis. The blue-colored yield values labeled refer to the **DO** fraction; (B) monomer and **DO** yield were obtained from different types of wood biomass; (C) DMBQ and 14CHDO yields were obtained from different wood biomass.

which is different from commercially available **14CHDA** with a 75 : 25 *cis/trans* ratio as also explained in more detail in ESI Note 4.† It is noteworthy to mention that *trans* **14CHDA** is more stable than *cis* **14CHDA**. Interestingly, a clear effect on the thermal behavior, such as melting temperature and crystal-

lization temperature, was evidenced with the use of the pure isomer for the preparation of polyamides.[26] After filtration and solvent removal, **14CHDA** was isolated in an 86% yield and characterized by ^{1}H NMR and ^{13}C NMR (Fig. S19 and S20†) (Fig. 5).
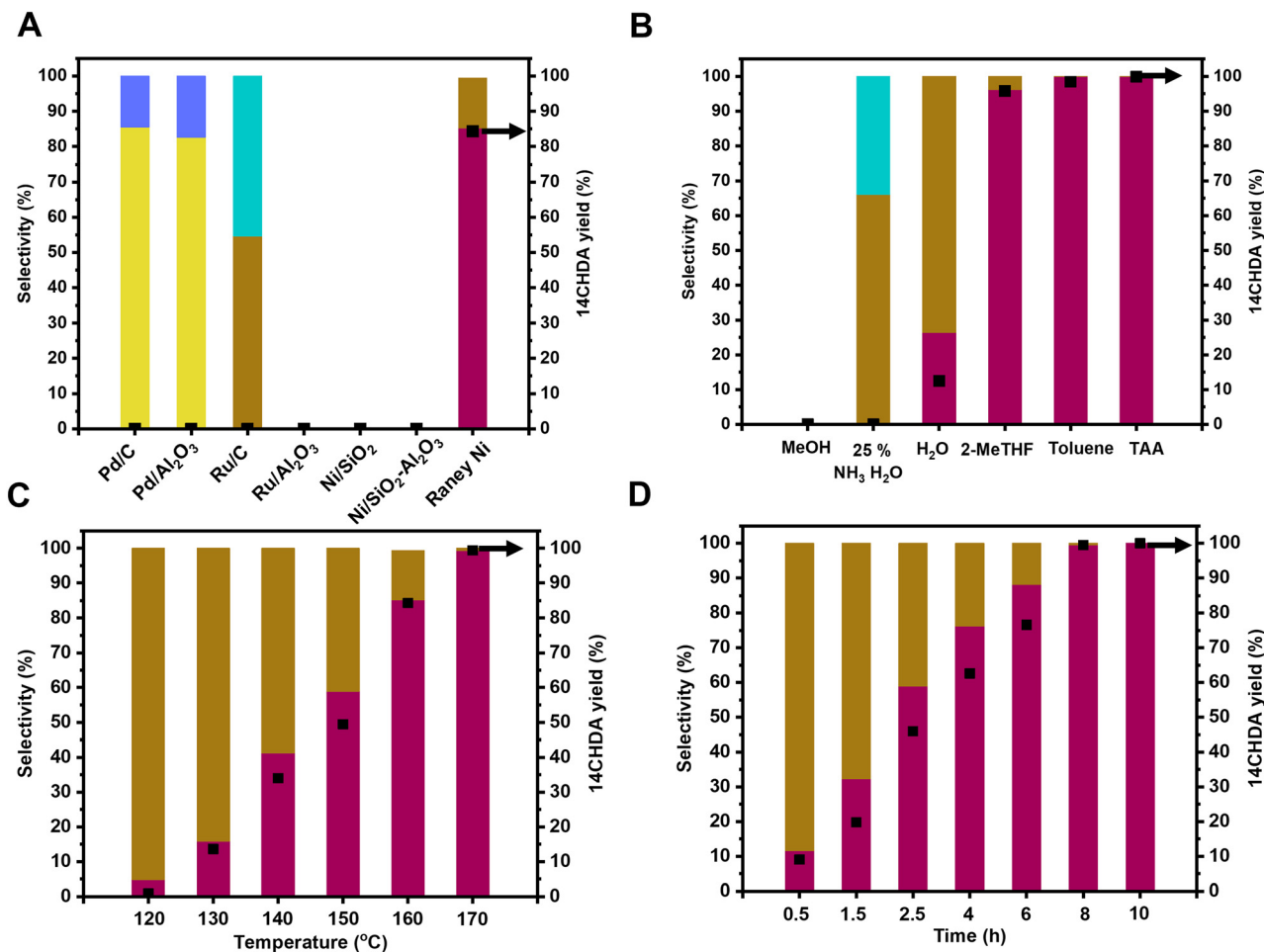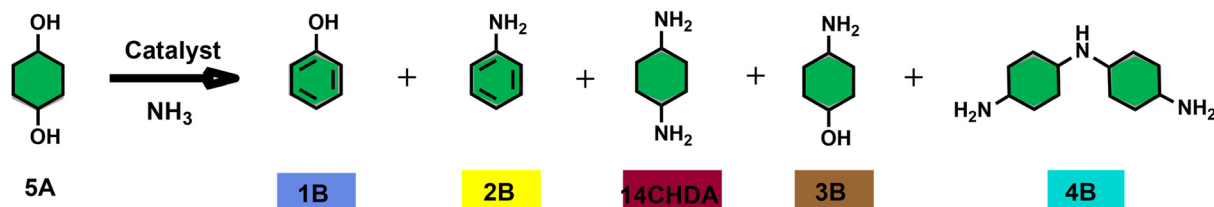
Fig. 5 Optimization of the reaction conditions for the catalytic conversion of 14CHDO to **14CHDA** (A–D); Unless otherwise specified, the standard reaction conditions are: 14CHDO (0.5 mmol), 100 mg catalyst, 2.5 mL solvent, 7 bar NH_3, 5 mg dodecane. (A) Screening of a range of commercially available heterogeneous metal catalysts at 160 °C for 3 h; (B) different solvents (150 °C, 8 h); (C) reaction temperature, 3 h; (D) reaction time, 150 °C; (A–D). Detailed numerical values are available in the ESI and more specifically in Tables S10–S13;† the conversion and yield values are determined by GC-FID using calibration curves and the internal standard; the black square in the figures refers to the **14CHDA** yield.

Conclusion

In conclusion, this work presents a catalytic strategy to valorize the hereto challenging RCF lignin-derived oligomeric fraction, featuring distinct C–C linkages, and convert it to industrially relevant 14CHDO and further on to **14CHDA**. To this end, this work takes maximum advantage of a previously developed procedure by the group of Samec for the conversion of the RCF lignin-derived oligomeric fraction into DMBQ—a new platform molecule derivable from lignin.[16] Additionally, it is concisely shown that commercially available RANEY® Ni can uniquely catalyze both the DMBQ to 14CHDO transformation and the

latter's diamination to **14CHDA**. This is an important finding as it provides a new sustainable route to a set of compounds, 14CHDO and **14CHDA**, which are both highly industrially relevant and cover a multitude of industries and applications. More specifically, this is achieved by a noble-metal-free catalytic procedure comprising of the following two steps: (a) the catalytic demethoxylation and hydrogenation of DMBQ into 14CHDO (86% yield) and (b) the quantitative catalytic direct amination of 14CHDO with ammonia to **14CHDA**. Most notably, these catalytic steps can all be conveniently catalyzed by RANEY® Ni—a true workhorse in the current chemical industry. Furthermore, this procedure is shown to be appli-

cable in the conversion of a wider range of oligomeric lignin streams, as generally present in crude (RCF) lignin oils. Overall, the here presented catalytic procedure is capable of transforming high molecular weight lignin oil of beech wood into 10.7 wt% of 14CHDO on a DO basis. It is noteworthy that the here developed methodology does not derive 14CHDO and **14CHDA** from petroleum-derived resources and in particular carcinogenic/mutagenic benzene, therefore providing another stride to a more sustainable chemical provision.

Conflicts of interest

The authors declare no competing interests.

Acknowledgements

References

1 C. O. Tuck, *Science*, 2012, **338**, 604–604.

2 Z. Sun, B. Fridrich, A. de Santi, S. Elangovan and K. Barta, *Chem. Rev.*, 2018, **118**, 614–678.

3 M. Pelckmans, T. Renders, S. Van de Vyver and B. Sels, *Green Chem.*, 2017, **19**, 5303–5331.

4 X. Chen, S. Song, H. Li, G. k. Gözaydın and N. Yan, *Acc. Chem. Res.*, 2021, **54**, 1711–1722.

5 J. He, L. Chen, S. Liu, K. Song, S. Yang and A. Riisager, *Green Chem.*, 2020, **22**, 6714–6747.

6 Y. Wang, S. Furukawa, X. Fu and N. Yan, *ACS Catal.*, 2019, **10**, 311–335.

7 S. S. Wong, R. Y. Shu, J. G. Zhang, H. C. Liu and N. Yan, *Chem. Soc. Rev.*, 2020, **49**, 5510–5560.

8 Z. H. Sun and K. Barta, *Chem. Commun.*, 2018, **54**, 7725–7745.

9 M. V. Galkin and J. S. Samec, *ChemSusChem*, 2016, **9**, 1544–1558.

10 W. Schutyser, T. Renders, S. Van den Bosch, S. F. Koelewijn, G. T. Beckham and B. F. Sels, *Chem. Soc. Rev.*, 2018, **47**, 852–908.

11 Z. R. Zhang, J. L. Song and B. X. Han, *Chem. Rev.*, 2017, **117**, 6834–6880.

12 M. M. Abu-Omar, K. Barta, G. T. Beckham, J. S. Luterbacher, J. Ralph, R. Rinaldi, Y. Roman-Leshkov, J. S. M. Samec, B. F. Sels and F. Wang, *Energy Environ. Sci.*, 2021, **14**, 262–292.

13 Y. M. Questell-Santiago, M. V. Galkin, K. Barta and J. S. Luterbacher, *Nat. Rev. Chem.*, 2020, **4**, 311–330.

14 T. Renders, G. Van den Bossche, T. Vangeel, K. Van Aelst and B. Sels, *Curr. Opin. Biotechnol.*, 2019, **56**, 193–201.

15 Y. M. Questell-Santiago, M. V. Galkin, K. Barta and J. S. Luterbacher, *Nat. Rev. Chem.*, 2020, **4**, 311–330.

16 E. Subbotina, T. Rukkijakan, M. D. Marquez-Medina, X. W. Yu, M. Johnsson and J. S. M. Samec, *Nat. Chem.*, 2021, **13**, 1118–1125.

17 T. Higuchi, C. Satake and M. Hirobe, *J. Am. Chem. Soc.*, 1995, **117**(34), 8879–8880.

18 S. Bian, C. Pagan, A. A. Andrianova and G. D. Du, *ACS Omega*, 2016, **1**, 1049–1057.

19 J. N. Asaad and S. L. Abd-El-Messieh, *J. Appl. Polym. Sci.*, 2008, **109**, 1916–1924.

20 J. I. Moon, Y. H. Lee and H. J. Kim, *Prog. Org. Coat.*, 2012, **74**, 125–133.

21 M. T. S. Rosado, T. M. R. Maria, R. A. E. Castro, J. Canotilho, M. R. Silva and M. E. S. Eusebio, *CrystEngComm*, 2014, **16**, 10977–10986.

22 A. M. Galal, W. Gul, D. Slade, S. A. Ross, S. Feng, M. G. Hollingshead, M. C. Alley, G. Kaur and M. A. ElSohly, *Bioorg. Med. Chem.*, 2009, **17**, 741–751.

23 G. Süss-Fink, G. B. Shul'pin and L. S. Shul'pina, Process for the production of ketones, EP1385812A1, 2004.

24 **https://www.chemicalbook.com/ChemicalProductProperty_EN_CB93336213.htm.**

25 K. H. Huang and G. H. He, New preparation process of 1,4-cyclohexanedione monoethylene acetal, CN102746269A, 2012.

26 B. Vanhaecht, B. Rimez, R. Willem, M. Biesemans and C. E. Koning, *J. Polym. Sci. Part A Polym. Chem.*, 2002, **40**, 1962–1971.

27 H. A. Lecomte, J. J. Liggat and A. S. G. Curtis, *J. Polym. Sci. Part A Polym. Chem.*, 2006, **44**, 1785–1795.

28 J. Ishii, S. Horii, N. Sensui, M. Hasegawa, L. Vladimirov, M. Kochi and R. Yokota, *High Perform. Polym.*, 2009, **21**, 282–303.

29 J. S. Santana, E. S. Cardoso, E. R. Triboni and M. J. Politi, *Polymers*, 2021, **13**, 4393.

30 H. Oertel, B. Zorn, W. Thoma and K. Noll, Polyurethane-ureas based on cis-trans-1,4-diaminocyclohexane, USRE29623E, 1978.

31 S. Wyllie, M. Thomas, S. Patterson, S. Crouch, M. De Rycker, R. Lowe, S. Gresham, M. D. Urbaniak, T. D. Otto, L. Stojanovski, F. R. C. Simeons, S. Manthri, L. M. MacLean, F. Zuccotto, N. Homeyer, H. Pflaumer, M. Boesche, L. Sastry, P. Connolly, S. Albrecht, M. Berriman, G. Drewes, D. W. Gray, S. Ghidelli-Disse, S. Dixon, J. M. Fiandor, P. G. Wyatt, M. A. J. Ferguson, A. H. Fairlamb, T. J. Miles, K. D. Read and I. H. Gilbert, *Nature*, 2018, **560**, 192–197.

32 C. M. Olson, B. Jiang, M. A. Erb, Y. Liang, Z. M. Doctor, Z. Zhang, T. Zhang, N. Kwiatkowski, M. Boukhali and J. L. Green, *Nat. Chem. Biol.*, 2018, **14**, 163–170.

33 G. L. Gist and J. R. Burg, *Toxicol. Ind. Health*, 1997, **13**, 661–714.

34 C. F. Huang and Y. H. Chou, Process for producing hydroquinone and derivates, US9630899B1, 2017.

35 H. X. Ma and J. G. Cai, *Russ. J. Appl. Chem.*, 2014, **87**, 397–403.

36 Y. J. Ding, T. Wang, Y. Lv and L. X. Ma, Method for preparing cyclohexanediamine through catalytic hydrogenation, CN102690204B, 2014.

37 Y. Z. Liu, A. Afanasenko, S. Elangovan, Z. H. Sun and K. Barta, *ACS Sustainable Chem. Eng.*, 2019, **7**, 11267–11274.

38 K. Shimizu, K. Kon, W. Onodera, H. Yamazaki and J. N. Kondo, *ACS Catal.*, 2013, **3**, 112–117.

39 Y. Kita, M. Kuwabara, S. Yamadera, K. Kamata and M. Hara, *Chem. Sci.*, 2020, **11**, 9884–9890.

40 K. Murugesan, T. Senthamarai, V. G. Chandrashekhar, K. Natte, P. C. J. Kamer, M. Beller and R. V. Jagadeesh, *Chem. Soc. Rev.*, 2020, **49**, 6273–6328.

41 A. Corma, J. Navas and M. J. Sabater, *Chem. Rev.*, 2018, **118**, 1410–1459.

42 J. He, L. L. Chen, S. M. Liu, K. Song, S. Yang and A. Riisager, *Green Chem.*, 2020, **22**, 6714–6747.

43 B. M. Stadler, C. Wulf, T. Werner, S. Tin and J. G. de Vries, *ACS Catal.*, 2019, **9**, 8012–8067.

44 V. Froidevaux, C. Negrell, S. Caillol, J. P. Pascault and B. Boutevin, *Chem. Rev.*, 2016, **116**, 14181–14224.

45 B. X. Zheng, J. L. Song, H. H. Wu, S. T. Han, J. X. Zhai, K. L. Zhang, W. Wu, C. Y. Xu, M. Y. He and B. X. Han, *Green Chem.*, 2021, **23**, 268–273.

46 B. Zhang, T. L. Guo, Y. X. Liu, F. E. Kuhn, C. Wang, Z. B. K. Zhao, J. L. Xiao, C. Z. Li and T. Zhang, *Angew. Chem., Int. Ed.*, 2021, **60**, 20666–20671.

47 H. Y. Zeng, D. W. Cao, Z. H. Qiu and C. J. Li, *Angew. Chem., Int. Ed.*, 2018, **57**, 3752–3757.

48 Z. W. Chen, H. Y. Zeng, H. Gong, H. N. Wang and C. J. Li, *Chem. Sci.*, 2015, **6**, 4174–4178.

49 T. Cuypers, T. Morias, S. Windels, C. Marquez, C. Van Goethem, I. Vankelecom and D. E. De Vos, *Green Chem.*, 2020, **22**, 1884–1893.

50 P. Zhang, T. B. Wu, M. Q. Hou, J. Ma, H. Z. Liu, T. Jiang, W. T. Wang, C. Y. Wu and B. X. Han, *ChemCatChem*, 2014, **6**, 3323–3327.

51 R. R. Deshmukh, J. W. Lee, U. S. Shin, J. Y. Lee and C. E. Song, *Angew. Chem., Int. Ed.*, 2008, **47**, 8615–8617.

52 X. Y. Wang and R. Rinaldi, *Energy Environ. Sci.*, 2012, **5**, 8244–8260.

53 G. Y. Bai, F. Li, X. X. Fan, Y. L. Wang, M. D. Qiu, Z. Ma and L. B. Niu, *Catal. Commun.*, 2012, **17**, 126–130.

54 M. Kennema, I. B. D. de Castro, F. Meemken and R. Rinaldi, *ACS Catal.*, 2017, **7**, 2437–2445.

55 X. Y. Wu, M. V. Galkin, T. Stern, Z. H. Sun and K. Barta, *Nat. Commun.*, 2022, **13**, 3376.

56 X. Y. Wu, M. V. Galkin and K. Barta, *Chem Catal.*, 2021, **1**, 1–14.